JOHANNES GUTENBERG UNIVERSITÄT MAINZ

PRISMA+

Pion-pole contribution to the muon g-2

Pion transition form factor from lattice QCD and experimental data

Danaheb Naomi Navarro Duran

MPA Summer School 2025, Chiemsee. September 2025

What is the Muon g-2?

One of the most compelling results in modern particle physics.

$$\boxed{\vec{\mu} = -g\frac{e}{2m}\vec{S}}$$

- According to the Dirac equation, $g = 2$ for fundamental leptons, with any discrepancy due to quantum corrections.

$$a_\mu = (g-2)/2 = a_\mu(\mathrm{QED}) + a_\mu(\mathrm{EW}) + a_\mu(\mathrm{hadronic})$$

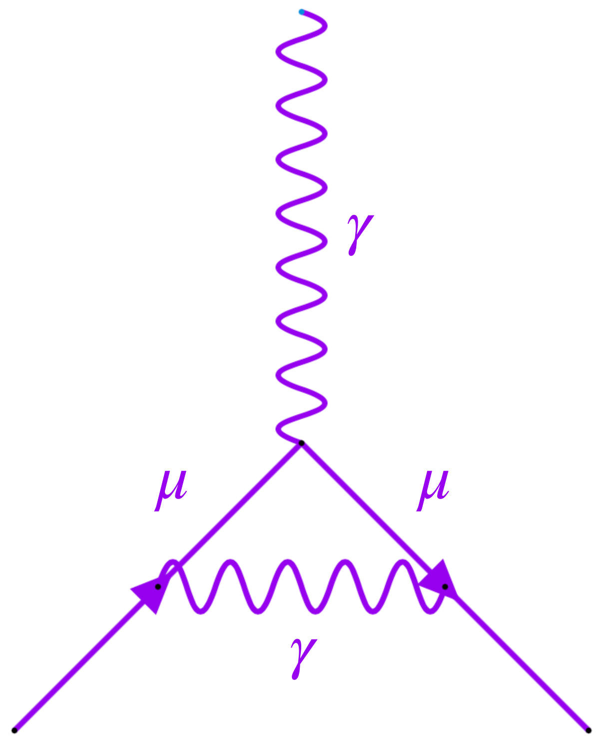

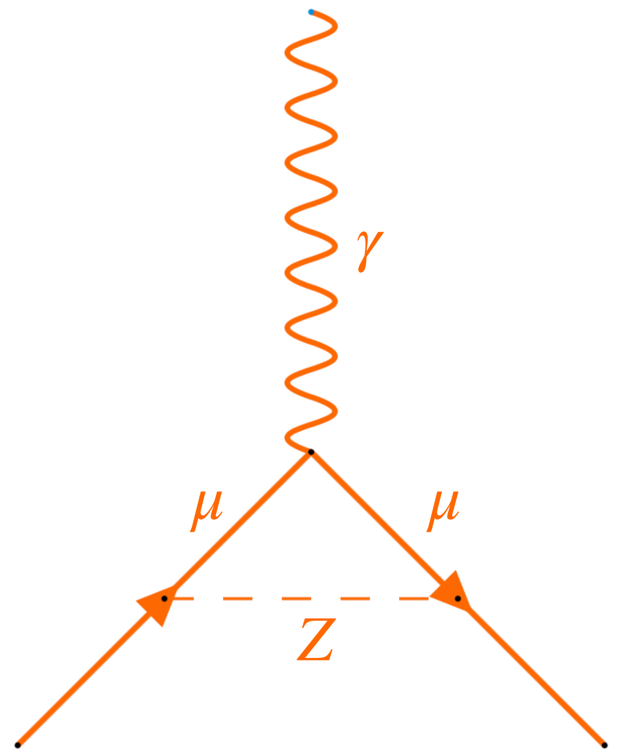

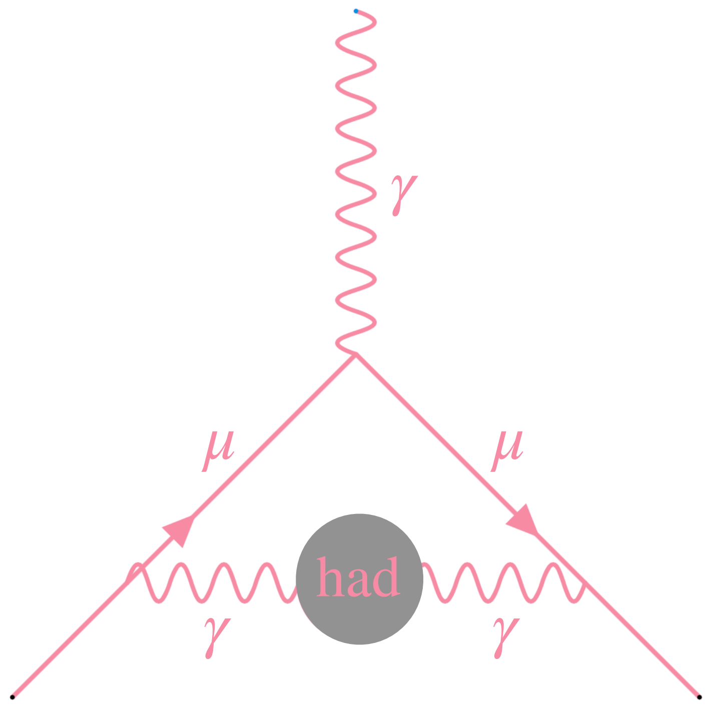

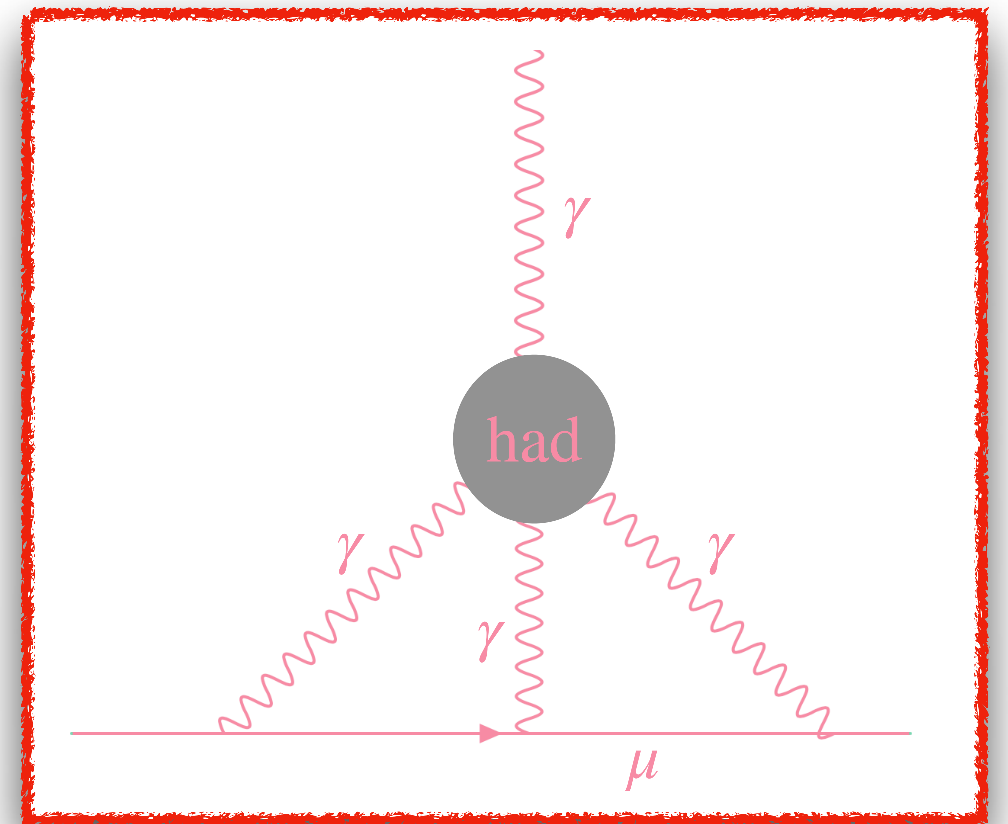

What is the Muon g-2?

One of the most compelling results in modern particle physics.

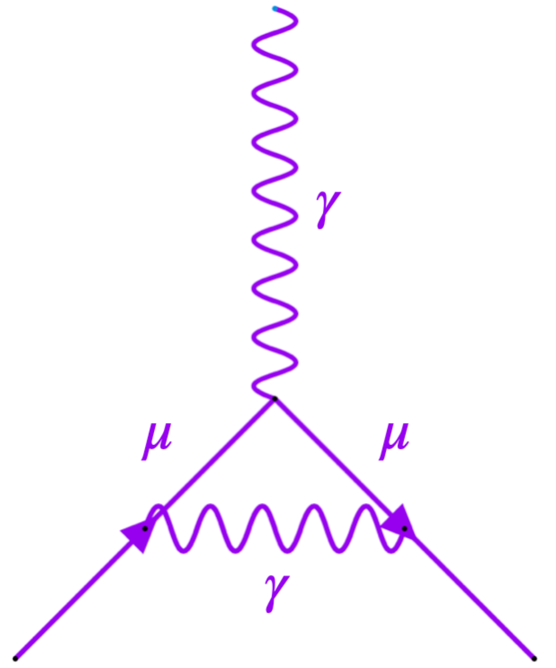

5 loop order

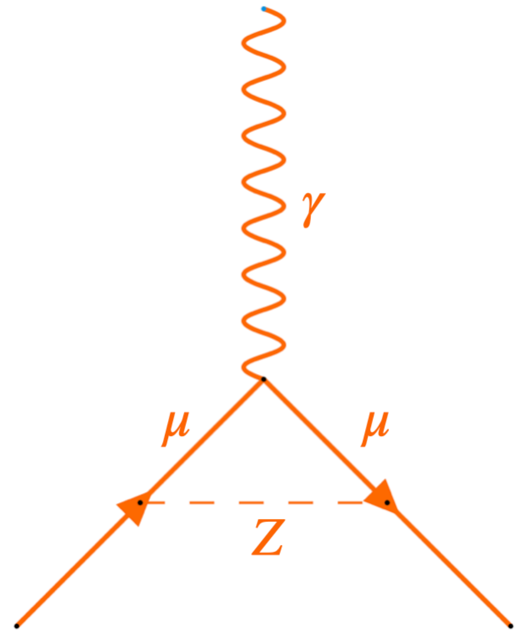

2 loop order

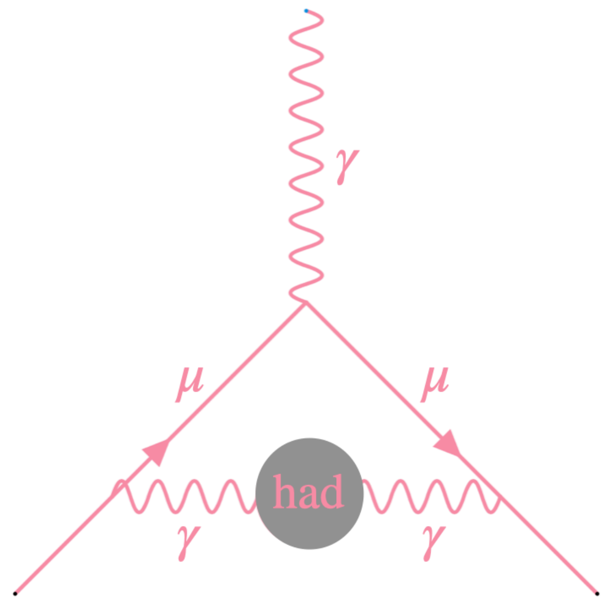

NNLO

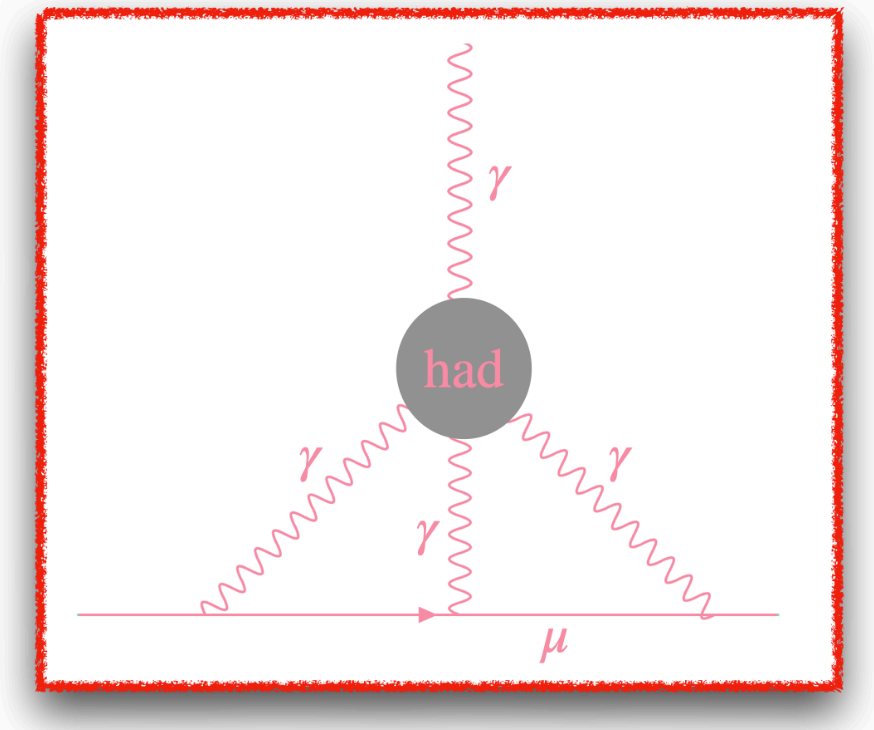

NLO

	DSE/BSE	WP20
π^0 exchange	62.6(1)(1.3)	$63.0^{+2.7}_{-2.1}$
η exchange	15.8(2)(3)(1.0)	16.3(1.4)
η' exchange	13.3(4)(3)(6)	14.5(1.9)
π^0, η, η' exchange	91.6(1.9)	$93.8^{+4.0}_{-3.6}$
π box	−15.7(2)(3)	−15.9(2)
K box	−0.48(2)(4)	−0.46(2)
π, K boxes/loops	−16.2(5)	−16.4(5)
S-wave $\pi\pi$ rescattering	–	−8.0(1.0)
higher scalar exchange	−1.6(5)	−2.0(2.0)
AV exchange (single)	17.4(6.0)	6.0(6.0)
AV exchange (tower) + SDC	24.8(6.1)	21.0(16.0)

White paper on the a_μ 2505.21476

Contribution	WP25	WP20
HVP LO (lattice)	7132(61)	7116(184)
HVP LO (e^+e^-, τ)	Table 5	6931(40)*
HVP NLO (e^+e^-)	−99.6(1.3)	−98.3(7)
HVP NNLO (e^+e^-)	12.4(1)	12.4(1)
HLbL (phenomenology)	103.3(8.8)	92(19)
HLbL NLO (phenomenology)	2.6(6)	2(1)
HLbL (lattice)	122.5(9.0)	82(35)
HLbL (phenomenology + lattice)	112.6(9.6)	90(17)
QED	116 584 718.8(2)	116 584 718.931(104)
EW	154.4(4)	153.6(1.0)
HVP (LO + NLO + NNLO)	7045(61)	6845(40)
HLbL (phenomenology + lattice + NLO)	115.5(9.9)	92(18)
Total SM Value	116 592 033(62)	116 591 810(43)

White paper on the a_μ 2505.21476

- Abs. uncertainty: HVP > HLbL
- Rel. uncertainty: HLbL > HVP

General Motivation

Pseudoscalar-pole contribution to the g-2

And its main and light character

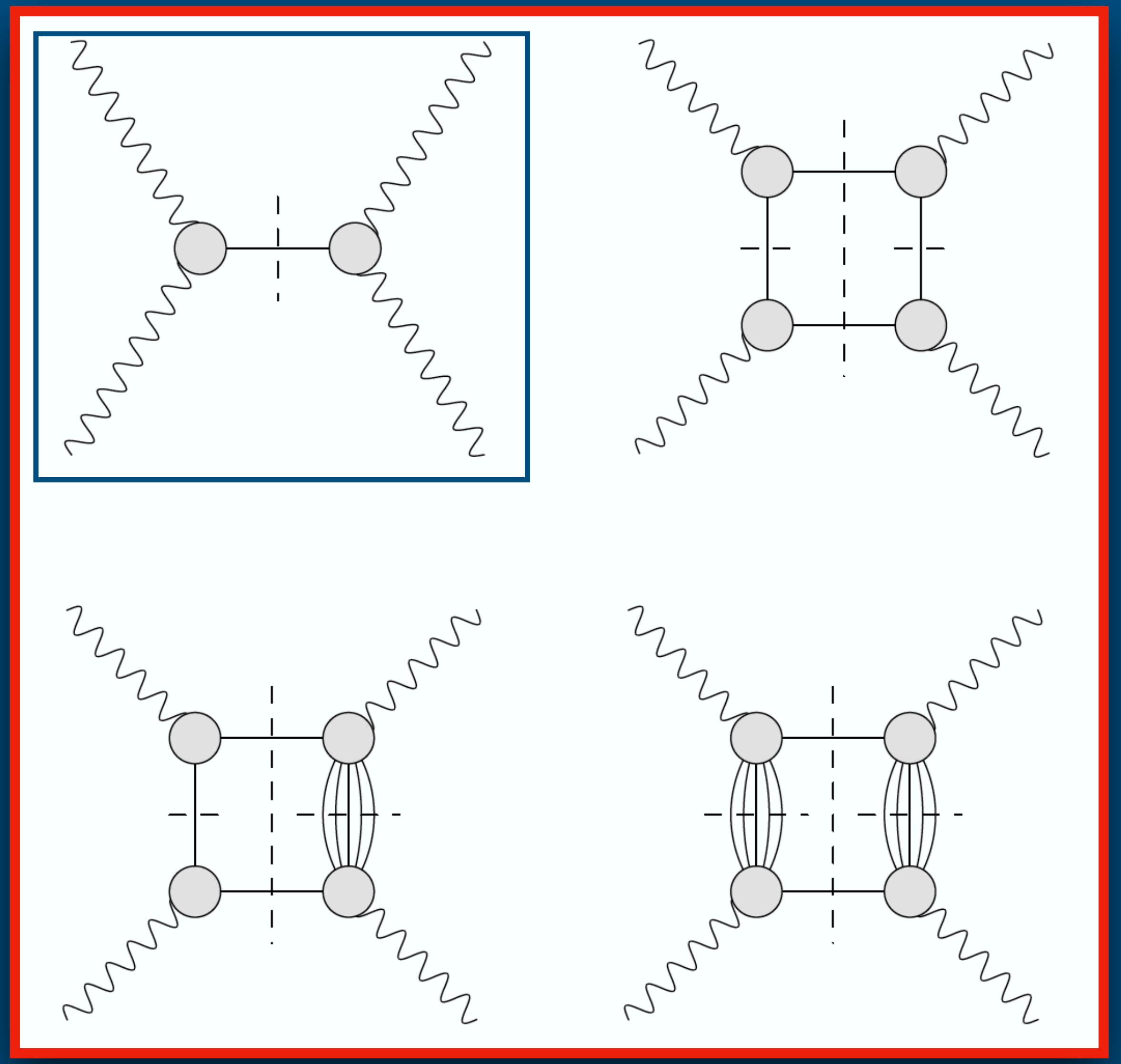

G. Colangelo et al ., JHEP 1509 (2015) 074

- Dispersive approaches apply **<u>different cuts</u>** to the amplitude.
- Systematic way to avoid **<u>double counting</u>**.
- **Pion-pole contribution**

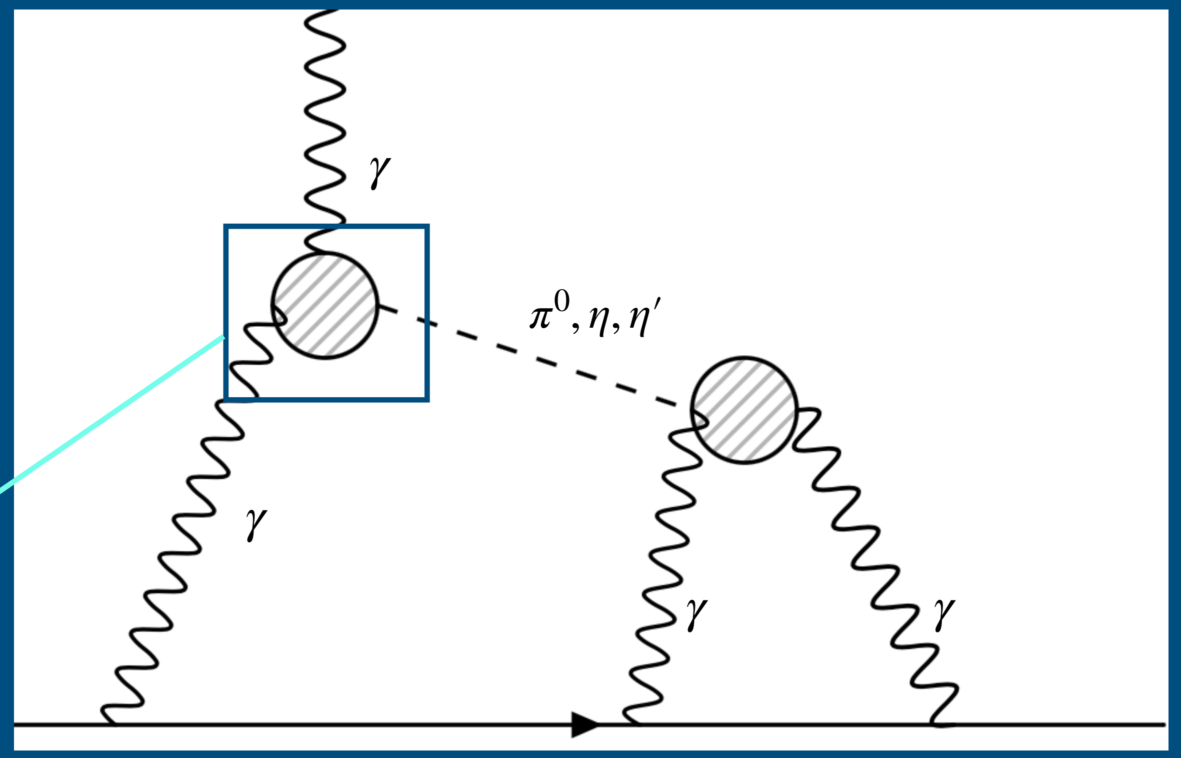

Transition form factor

$$M_{\mu\nu}(q_1, q_2) = \epsilon_{\mu\nu\alpha\beta} q_1^\alpha q_2^\beta F_{\pi^0\gamma^*\gamma^*}(-q_1^2, -q_2^2)$$

Describe the interaction between a pseudoscalar meson (e.g., the pion) and two (virtual) photons

Transition form factor of the pion (π^0 TFF)

Bridging the gap between theory and experiment.

- How the π^0 TFF is obtained?
- Experimental data for the single-virtual πTFF from CELLO, CLEO, BABAR, Belle and recently from BESIII

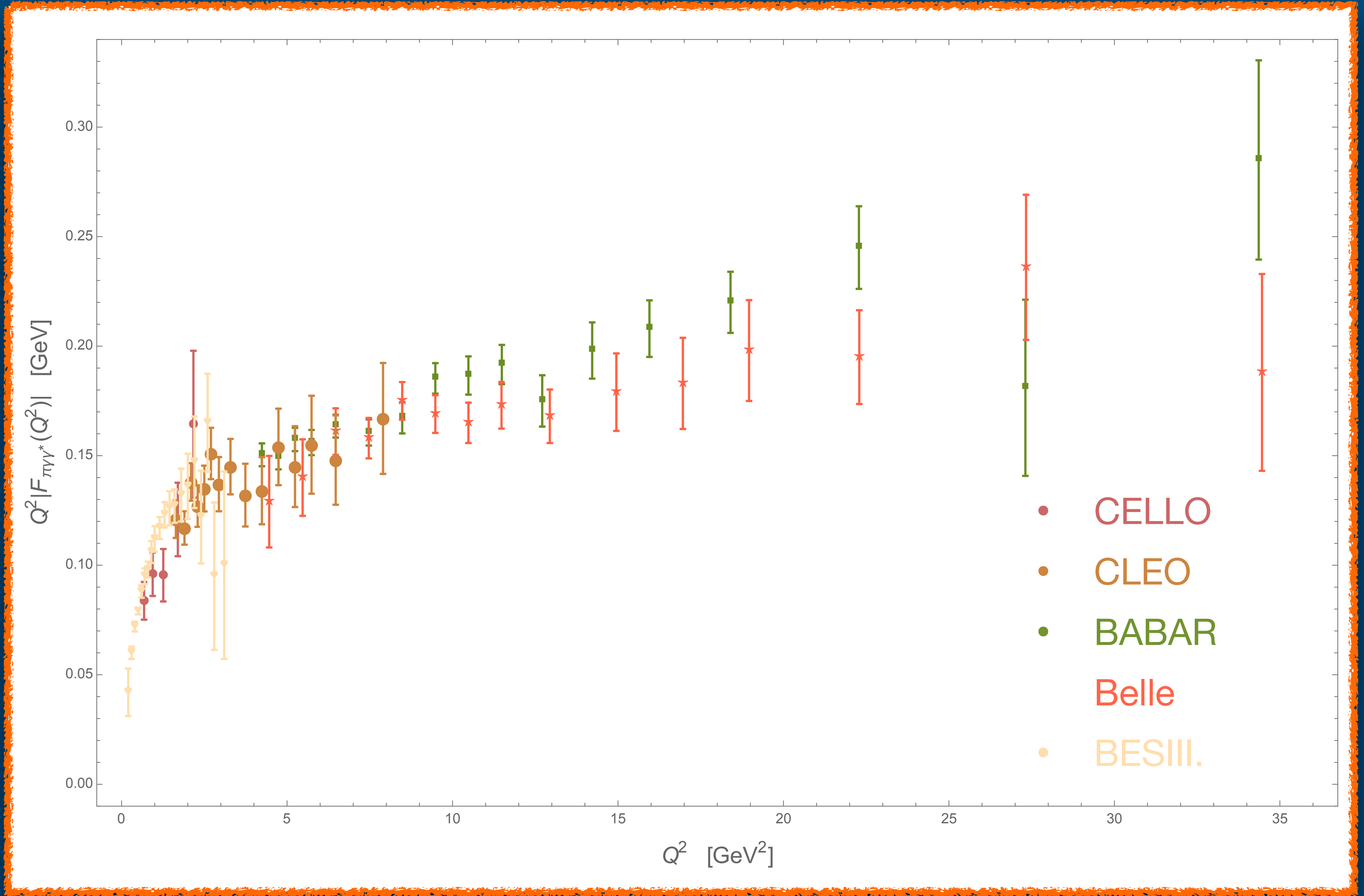

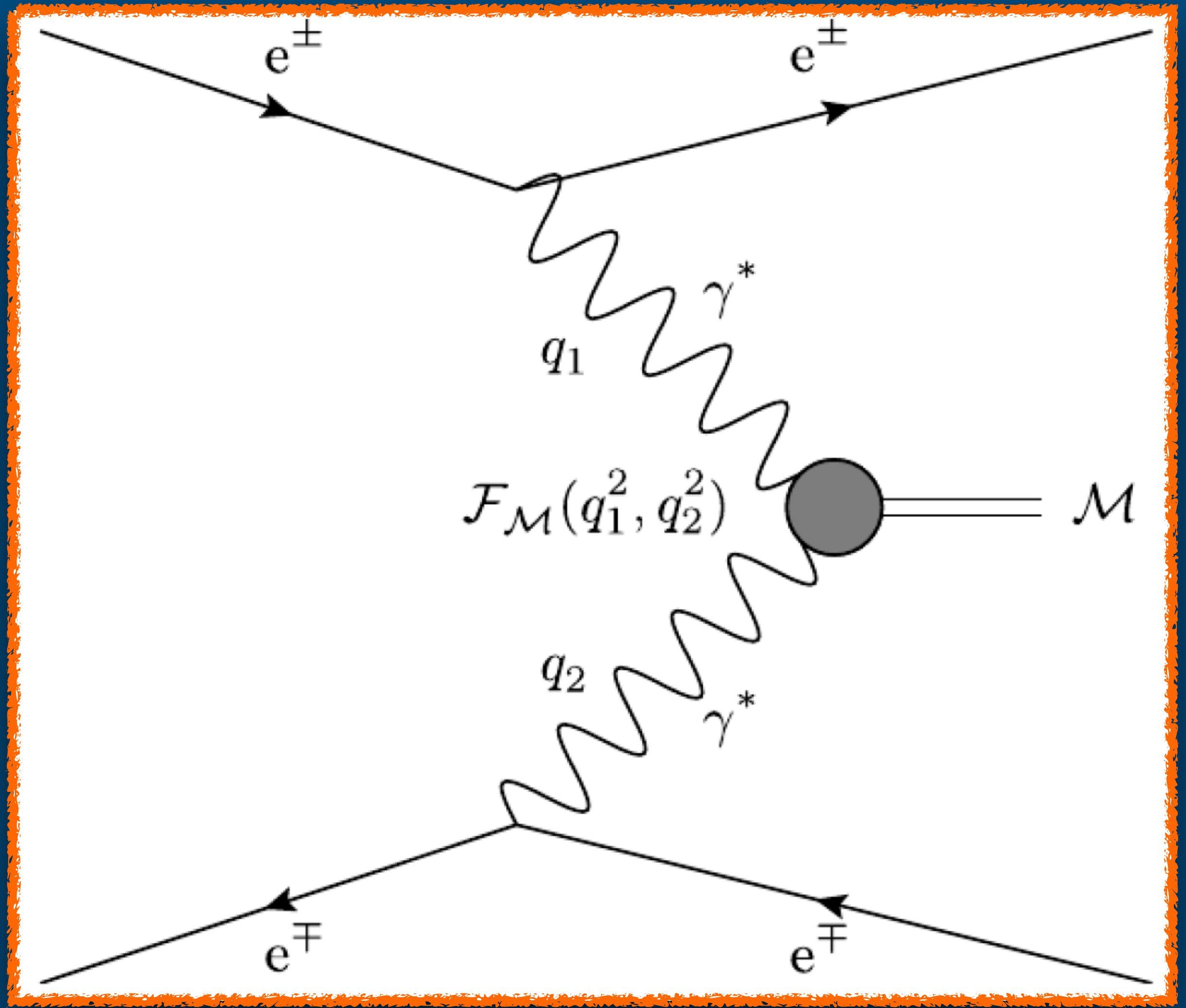

C. Redmer. 8th plenary Workshop of the muon g-2 Theo. Initiative

- New BES-III data: 20 data points in the region of 0.2 to 3.5 GeV^2
- Lattice QCD data.

Lattice QCD (LQCD)

And how to be left with *squared eyes*.

Id	a	$\tilde{y} = m_\pi^2/(16\pi^2 f_\pi^2)$	N
J303	0.0498095	0.0494863	5197
N300		0.132283	2694
D200	0.0642606	0.0295507	7514
N200		0.0597152	3248
N203		0.088836	3196
N202		0.125027	3075
N401	0.0763401	0.0606218	7014
S400		0.0905882	2847
C101	0.0863609	0.037344	3335
N101		0.0580176	7513
H102		0.0930381	3200
H101		0.128415	1670

A. Gérardin, H. Meyer, A. Nyffeler 1903.09471

- Non-perturbative method for solving QCD
- Finite lattice spacing “a”.
- Different masses for the pion. Not the physical *real* mass.

Transition form factor of the pion (π^0 TFF)

Lattice QCD vs everyone else?

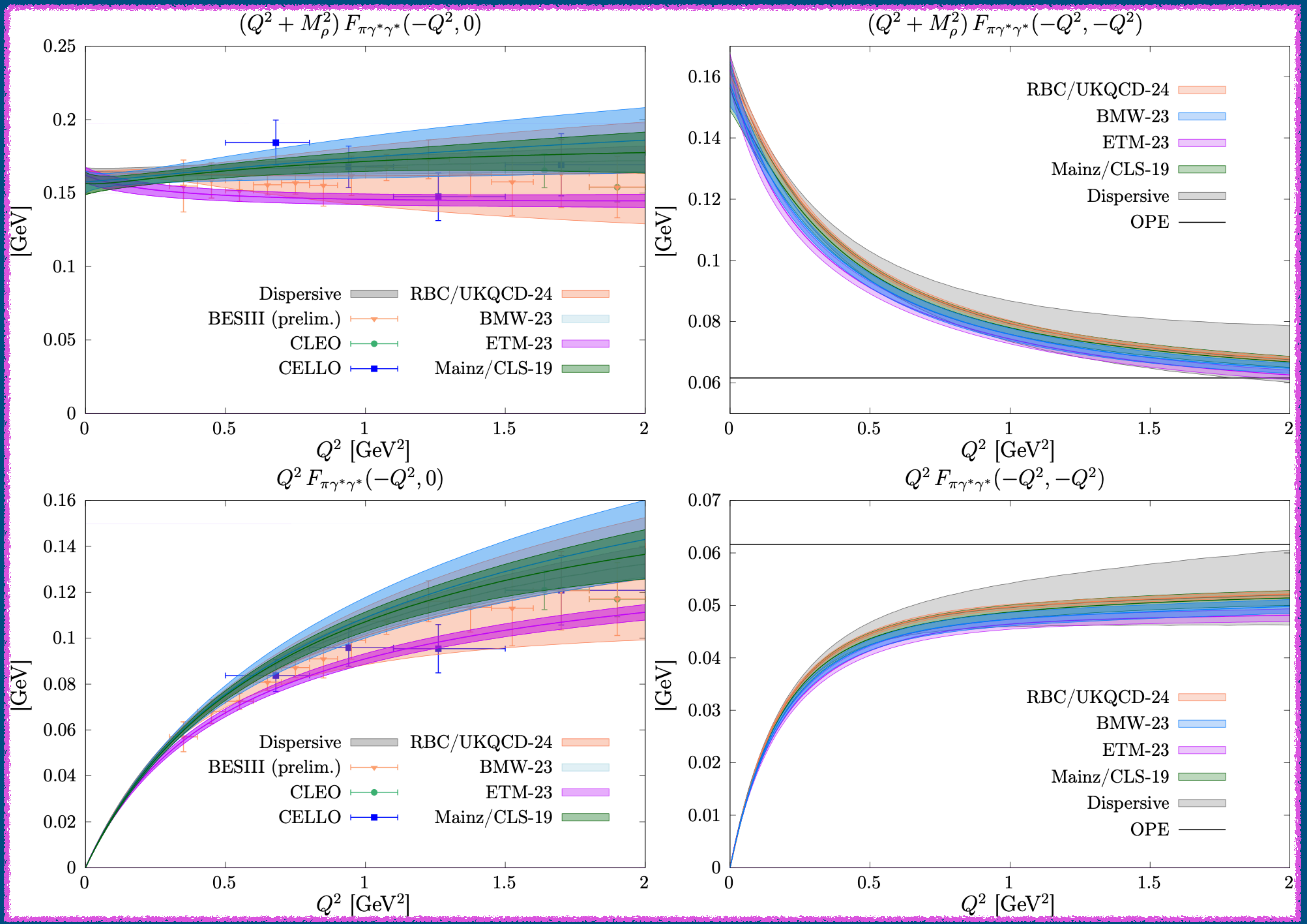

White paper on the a_μ 2505.21476

- ***Our* motivation**

A Unified Approach: Combining Data Sets

What works better in each region?

- ***Our* motivation**

- **Combine** LQCD and experimental data to **reduce the systematic and extrapolation** uncertainty.

- **Lattice** gives smaller uncertainty in a **double-virtual** region.

- **Experimental data** works great in the **single-virtual** region.

Asymptotic constraints on the TFF:

Constraints from the TFF

From virtual to real photons.

Asymptotic constraints on the TFF:

- Chiral anomaly: $$F_{\pi^0\gamma\gamma}(0,0) \longrightarrow \frac{1}{4\pi^2 f_\pi}$$
- Double-virtual form factor from operator product expansion (OPE): $$\lim_{Q^2\to\infty} F_{\pi^0\gamma^*\gamma^*}(Q^2, Q^2) = \frac{2f_\pi}{3}\left[\frac{1}{Q^2}\right]$$
- The single-virtual form factor exhibits the Brodsky–Lepage behavior: $$\lim_{Q^2\to\infty} F_{\pi^0\gamma^*\gamma}(Q^2,0) = \frac{2f_\pi}{Q^2}$$

Ansatz to the πTFF in Lattice QCD

From lattice simulations to phenomenological insights.

- The **LMD+V** model refines the **LMD** model by adding an extra vector resonance.

- It fulfils the **Brodsky-Lepage constraint** when $\tilde{h}_1 = 0$ and the **OPE constraint.**

$$\mathcal{F}^{\mathrm{LMD+V}}_{\pi^0\gamma^*\gamma^*}(Q_1^2, Q_2^2) = \frac{-\tilde{h}_0 Q_1^2 Q_2^2 (Q_1^2 + Q_2^2) + \tilde{h}_1 (Q_1^2 + Q_2^2)^2 + \tilde{h}_2 Q_1^2 Q_2^2 - \tilde{h}_5 M_{V_1}^2 M_{V_2}^2 (Q_1^2 + Q_2^2) + \alpha M_{V_1}^4 M_{V_2}^4}{(M_{V_1}^2 + Q_1^2)(M_{V_2}^2 + Q_1^2)(M_{V_1}^2 + Q_2^2)(M_{V_2}^2 + Q_2^2)}$$

A. Nyffeler 0203243

- All **free parameters** can be fitted considering $\tilde{h}_0 = -F_\pi/3$.

- In the **single-virtual** the **parameters to fit** are h_5, α, M_{V_1}
  - For extrapolate to the physical point one uses a $h_i(y, a)$ model.

Fit methodology and results: Methods A and B

And how to go from a model to measurement.

- Fit **individual** ensembles and all of them **together**

$$\mathcal{F}^{\mathrm{LMD+V}}_{\pi^0\gamma^*\gamma^*}(Q_1^2, Q_2^2) = \frac{-\tilde{h}_0 Q_1^2 Q_2^2 (Q_1^2 + Q_2^2) + \tilde{h}_2 Q_1^2 Q_2^2 - \tilde{h}_5 M_{V_1}^2 M_{V_2}^2 (Q_1^2 + Q_2^2) + \alpha M_{V_1}^4 M_{V_2}^4}{(M_{V_1}^2 + Q_1^2)(M_{V_2}^2 + Q_1^2)(M_{V_1}^2 + Q_2^2)(M_{V_2}^2 + Q_2^2)}$$

Knech and Nyffeler, PRD 65 (2002) 073034

- $\tilde{h}_0, \tilde{h}_2, \tilde{h}_5, \alpha, M_{V_1}$
- $M_{V_2}(y, a) = M_{V_1}(y, a) + 1.465 \text{ GeV} - 0.775 \text{ GeV}$

1. Fit each ensemble separately $\rightarrow h_i(a, y), \alpha(a, y), M_{V_1}(a, y)$
2. Fit experimental data separately $\rightarrow h_5(0, y_{phys}), \alpha(0, y_{phys}), M_{V_1}(0, y_{phys})$

Fit methodology and results: Method A.

And how to go from a model to measurement.

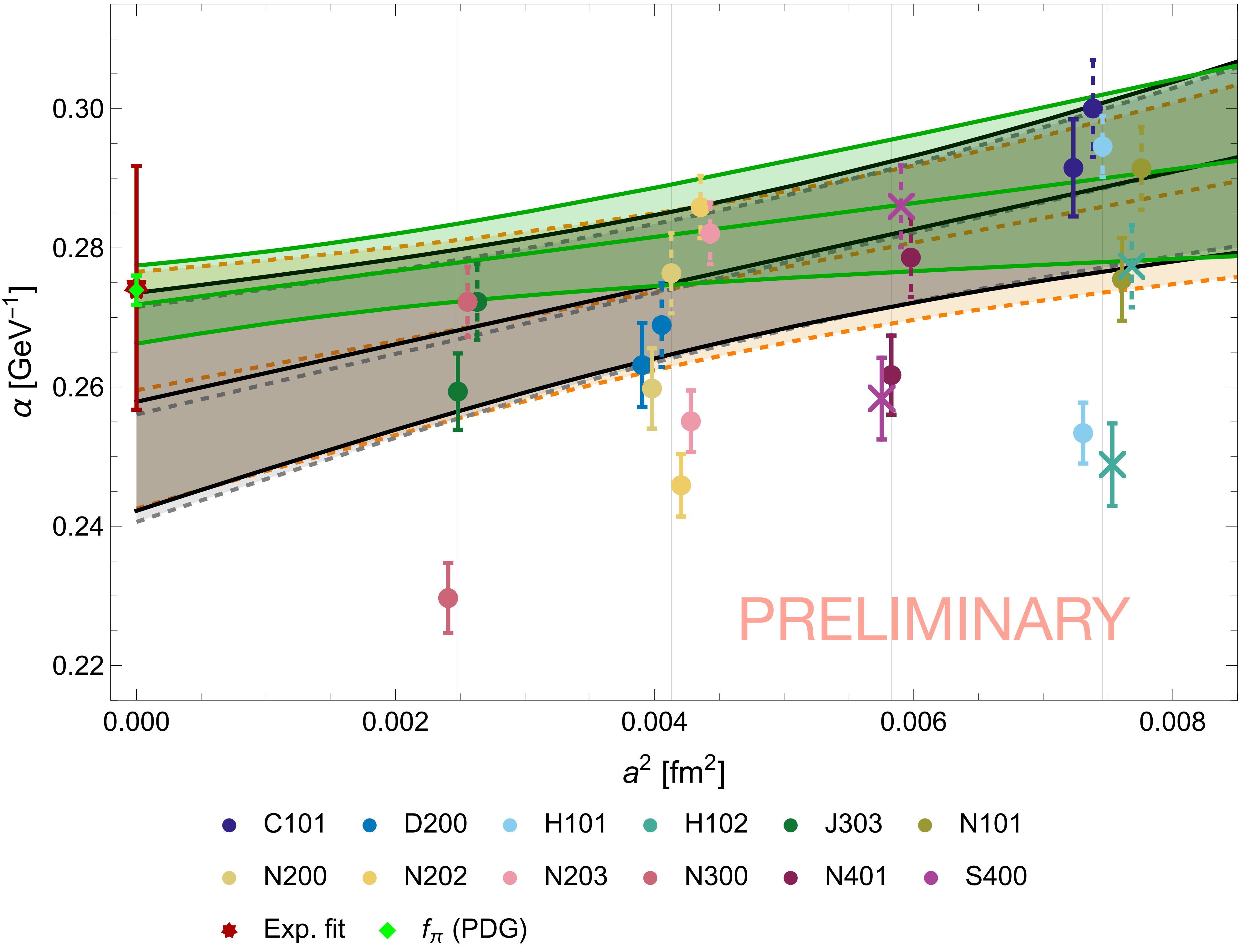

- Fit **individual** ensembles and all of them together

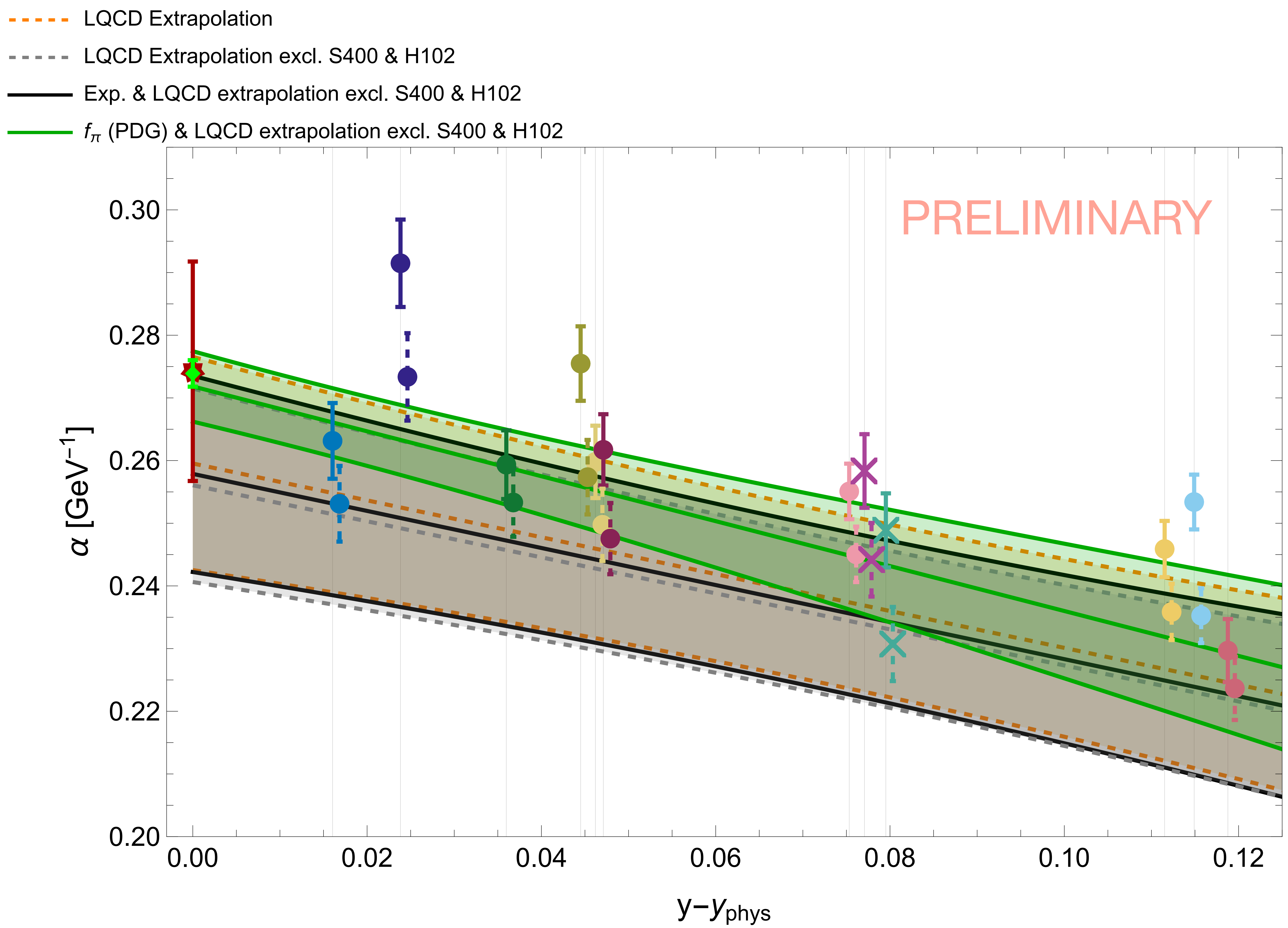

- Parameter α extrapolated to physical point.

Fit methodology and results: Method A.

And how to go from a model to measurement.

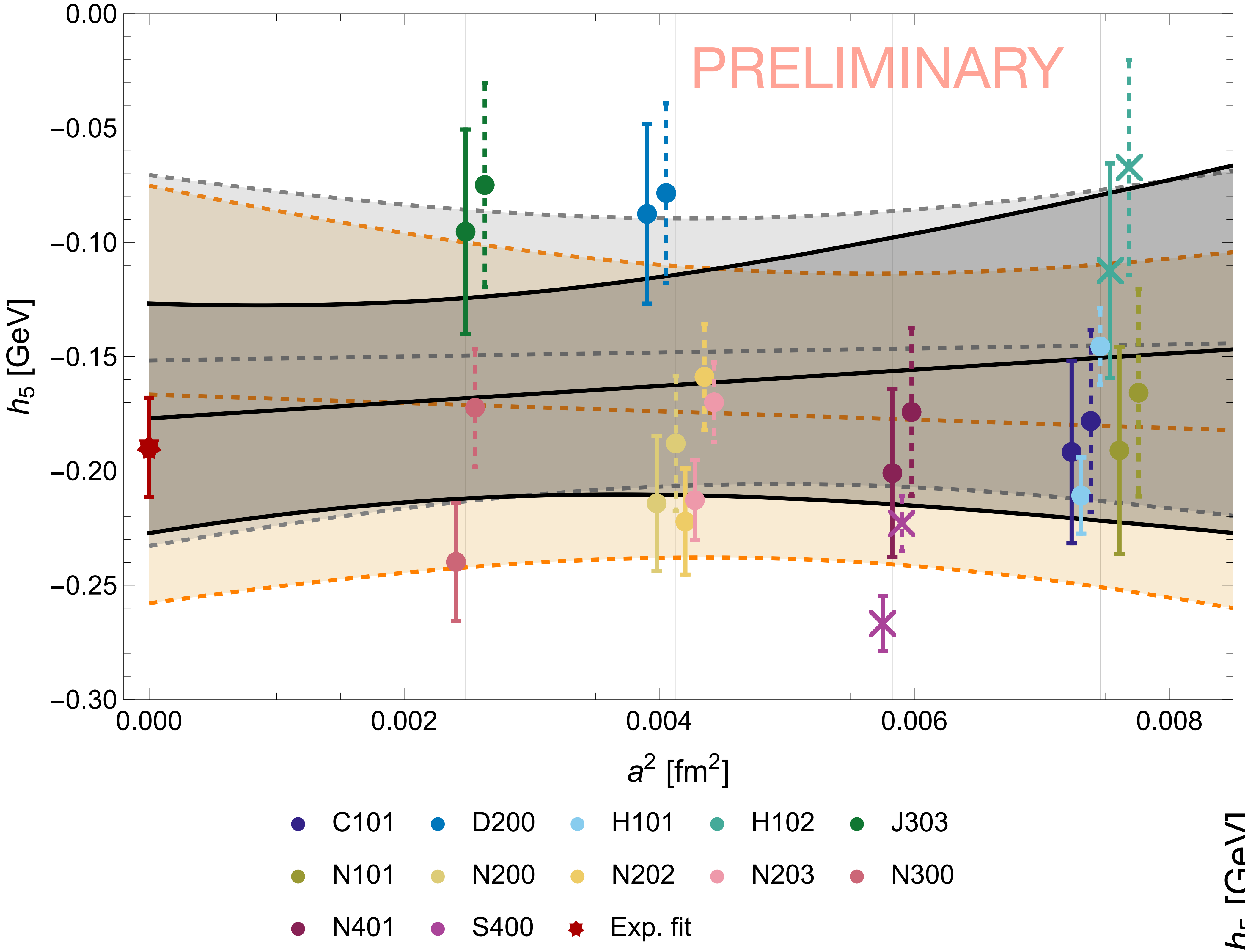

- Fit **individual** ensembles and all of them together

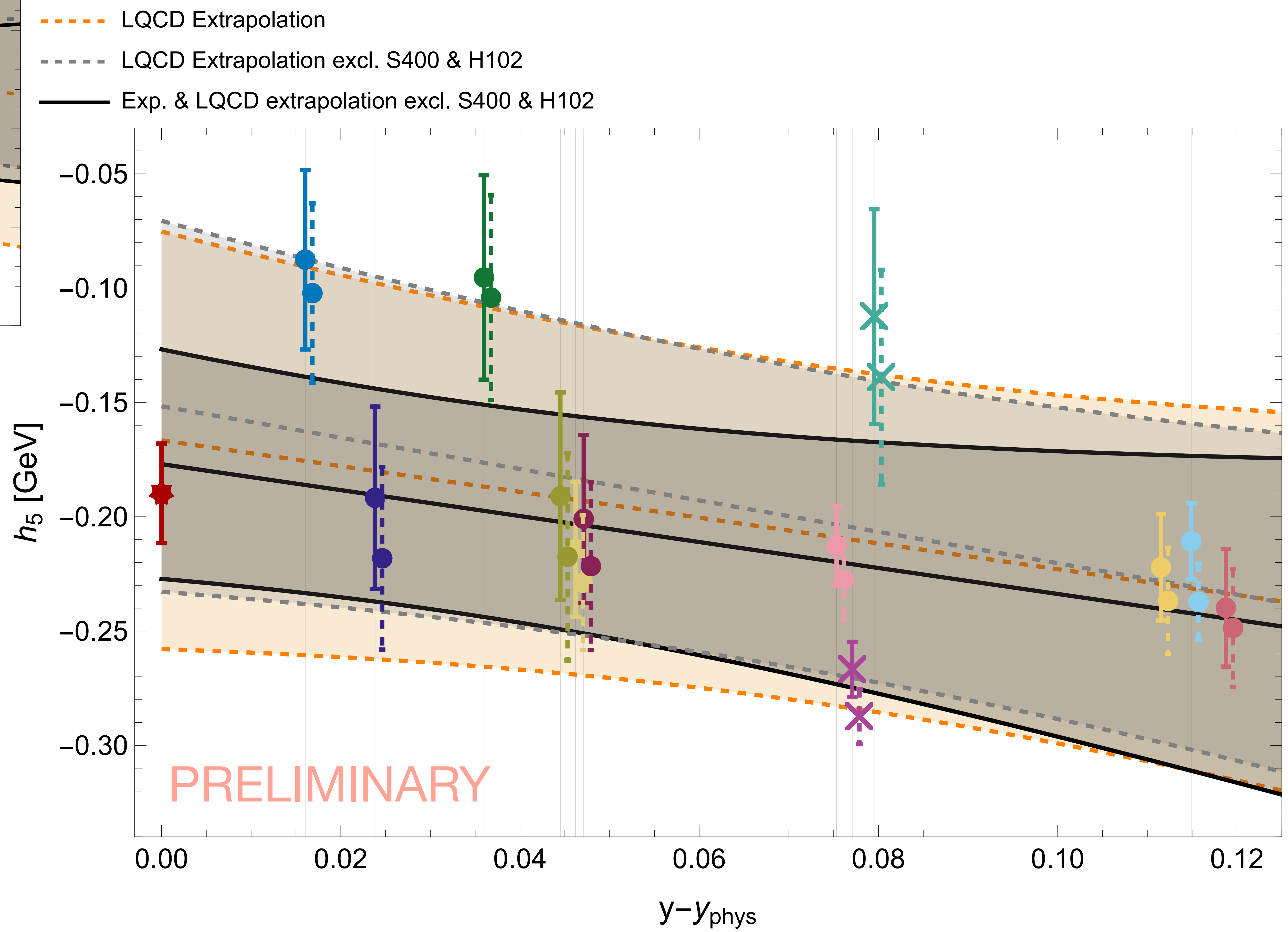

- Parameter h_5 extrapolated to physical point.

Fit methodology and results: Method B

And how to go from a model to measurement.

- Fit individual ensembles and all of them **together**

$$\mathcal{F}^{\mathrm{LMD+V}}_{\pi^0\gamma^*\gamma^*}(Q_1^2, Q_2^2) = \frac{-\tilde{h}_0 Q_1^2 Q_2^2 (Q_1^2 + Q_2^2) + \tilde{h}_2 Q_1^2 Q_2^2 - \tilde{h}_5 M_{V_1}^2 M_{V_2}^2 (Q_1^2 + Q_2^2) + \alpha M_{V_1}^4 M_{V_2}^4}{(M_{V_1}^2 + Q_1^2)(M_{V_2}^2 + Q_1^2)(M_{V_1}^2 + Q_2^2)(M_{V_2}^2 + Q_2^2)}$$

A. Nyffeler 0203243

- Fit all ensembles (and experimental data) together. $\rightarrow \vec{p}(0,y_{phys}), \overrightarrow{C}_a, \overrightarrow{C}_y$

- Extrapolation to the **physical point**.

$$\vec{p}(\tilde{y}, a) = \vec{p}(0, 0) + \overrightarrow{C}_y(y, y^{\mathrm{phys}}) + \overrightarrow{C}_a \left(\frac{a}{a_{\beta=5.3}}\right)^2$$

- $\underbrace{15 - 2 \text{ parameters}}_{M_{V_1} \text{ and } \tilde{h}_0}$ = **13 left as free parameters.***

* Could not subtract the parameters, it is a choice

Fit methodology and results: Method B.

And how to go from a model to measurement.

- Fit individual ensembles and all of them **together**

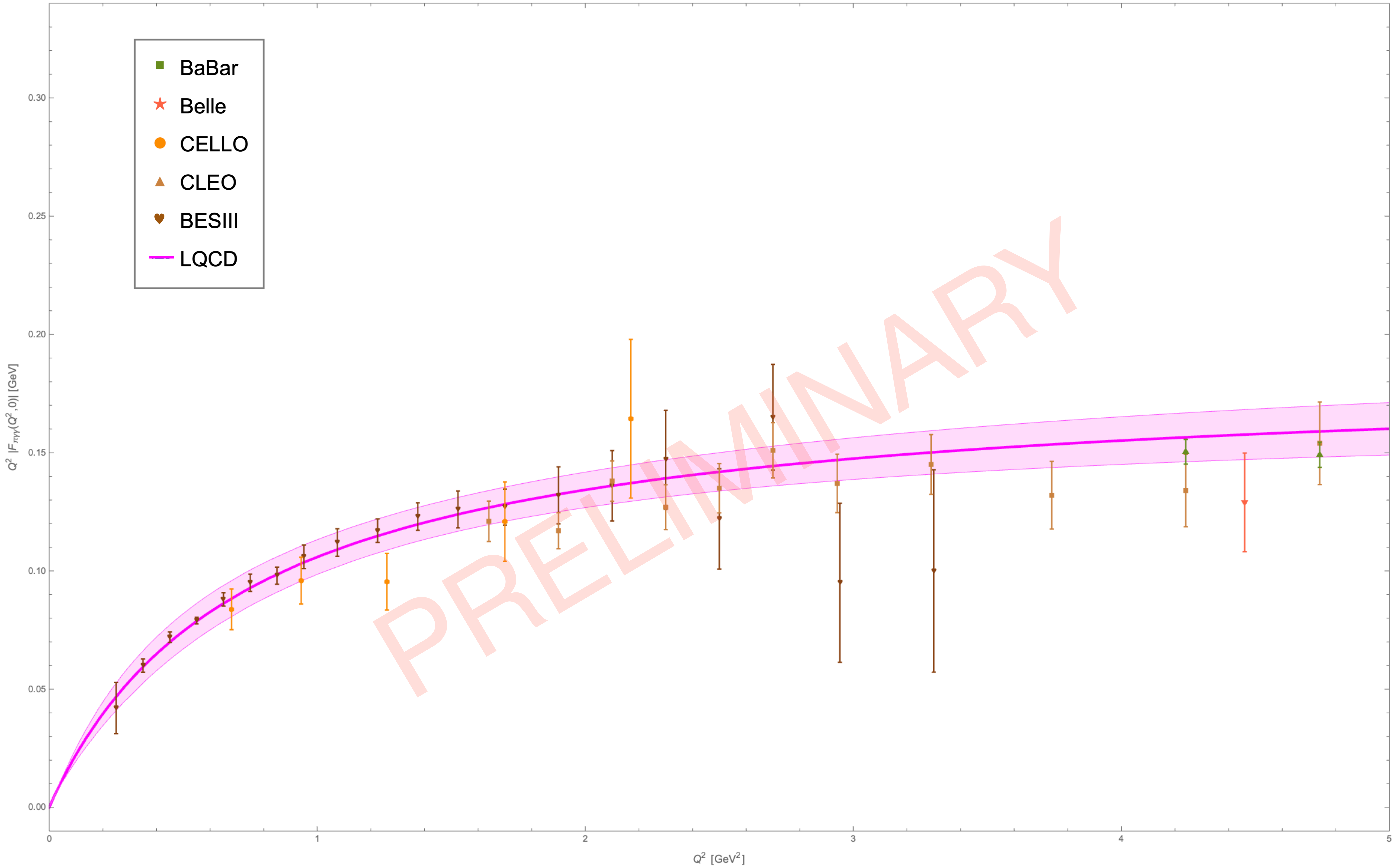

- Lattice QCD and experimental data agree, so this approach is **feasible**.

Fit methodology and results: Uncertainties

And how to go from a model to measurement.

- Fit **individual** ensembles and all of them **together.**
- One has **statistical** and **systematic** uncertainty.

	DSE/BSE	WP20
π^0 exchange	62.6(1)(1.3)	$63.0^{+2.7}_{-2.1}$
η exchange	15.8(2)(3)(1.0)	16.3(1.4)
η' exchange	13.3(4)(3)(6)	14.5(1.9)
π^0, η, η' exchange	$\boxed{91.6(1.9)}$	$93.8^{+4.0}_{-3.6}$
π box	−15.7(2)(3)	−15.9(2)
K box	−0.48(2)(4)	−0.46(2)
π, K boxes/loops	−16.2(5)	−16.4(5)
S-wave $\pi\pi$ rescattering	–	−8.0(1.0)
higher scalar exchange	−1.6(5)	−2.0(2.0)
AV exchange (single)	17.4(6.0)	6.0(6.0)
AV exchange (tower) + SDC	24.8(6.1)	21.0(16.0)

- Having LQCD and experimental data one can **fit them simultaneously** and reduce the systematical and extrapolation uncertainty from the a_μ.

Pseudoscalar-pole contribution to a_μ

And how mesons influence high-precision tests of the SM.

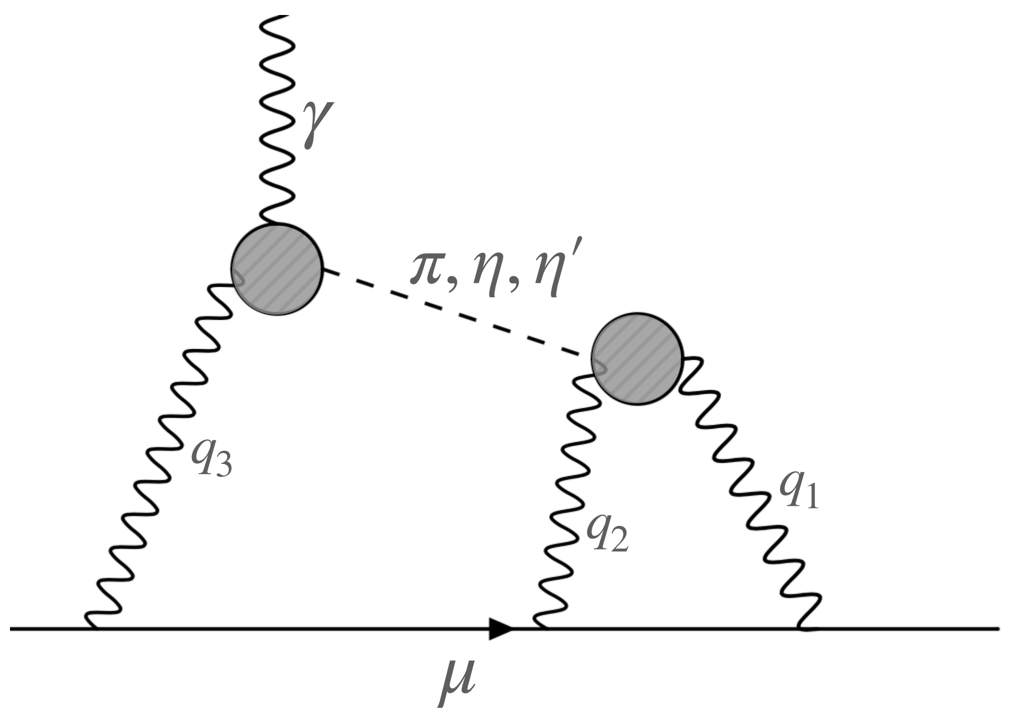

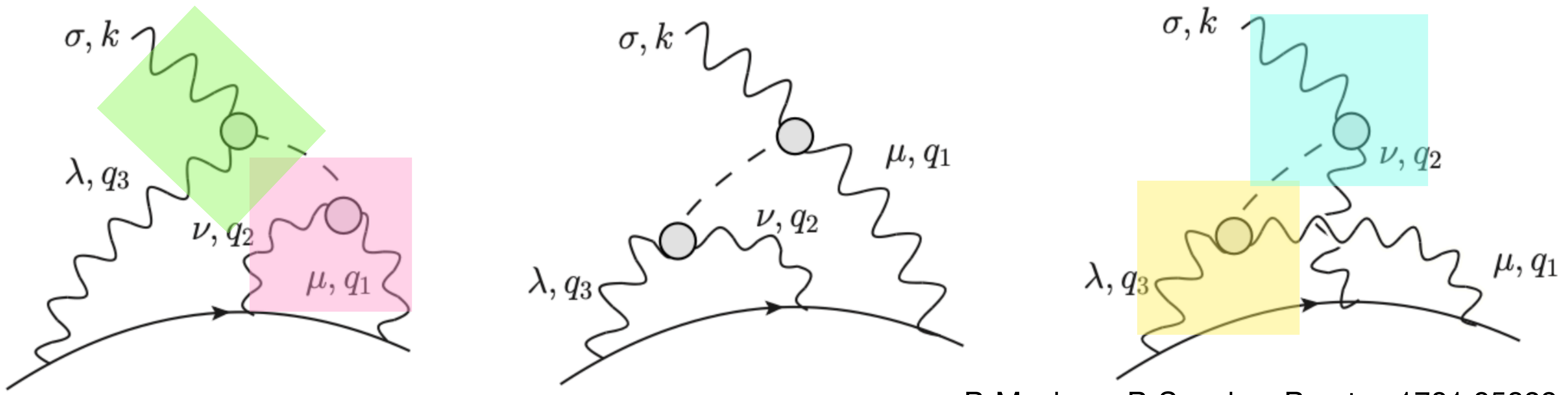

P. Masjuan, P. Sanchez Puertas 1701.05829

	Dispersive [37, 56, 550, 552]	CA [35]	RχT [50]	hQCD [47]	DSE/BSE [38]
π^0	$63.0^{+2.7}_{-2.1}$	63.6(2.7)	$61.3^{+2.5}_{-1.6}$	63.4(2.7)	62.6(1.3)
η	14.7(9)	16.3(1.4)	$15.2^{+1.2}_{-0.9}$	17.6(1.7)	15.8(1.1)
η'	13.5(7)	14.5(1.9)	$14.2^{+1.6}_{-1.1}$	14.9(2.0)	13.3(8)
Sum	$91.2^{+2.9}_{-2.4}$	94.4(3.6)	$91.3^{+3.2}_{-2.1}$	95.9(3.8)	91.6(1.9)

White paper on the a_μ 2505.21476

- Pion-pole contribution to HLbL.

$$a_\mu^{\mathrm{HLbL};\pi^0} = \left(\frac{\alpha}{\pi}\right)^3 \int_0^\infty dq_1 \int_0^\infty dq_2 \int_{-1}^{1} d\tau \, \Big(w_1(q_1, q_2, \tau)\, \mathcal{F}_{\pi^0\gamma^*\gamma^*}(q_1^2, q_3^2)\, \mathcal{F}_{\pi^0\gamma^*\gamma}(q_2^2, 0) + w_2(q_1, q_2, \tau)\, \mathcal{F}_{\pi^0\gamma^*\gamma^*}(q_1^2, q_2^2)\, \mathcal{F}_{\pi^0\gamma^*\gamma}(q_3^2, 0) \Big)$$

What's next?

How might this research be taken further?

- Combined fit of lattice and experimental data (Method B)
- Study impact of TFF improvements on a_μ
- Consider ansatz with more parameters in singly-virtual kinematics: conformal fit or Canterbury approximants.
- NNLO ChPT fit (Bickert et al, PhysRevD.102.074019)
- Extension to η, η' with existing experimental data for doubly-virtual kinematics

Thank you!

Questions are happily received(:

Backupslides

The Jackknife Standard Error is defined

$$SE(\hat{\theta})_{jack} = \left\{\frac{n-1}{n}\sum_{i=1}^{n}(\hat{\theta}_{(i)} - \hat{\theta}_{(\cdot)})^2\right\}^{1/2},$$

where $\hat{\theta}_{(\cdot)}$ is the empirical average of the Jackknife replicates:

$$\hat{\theta}_{(\cdot)} = \frac{1}{n}\sum_{i=1}^{n}\hat{\theta}_{(i)}$$

Lattice QCD: kinematical reach

And how to be left with *squared eyes*.

- Kinematical reach is definite.

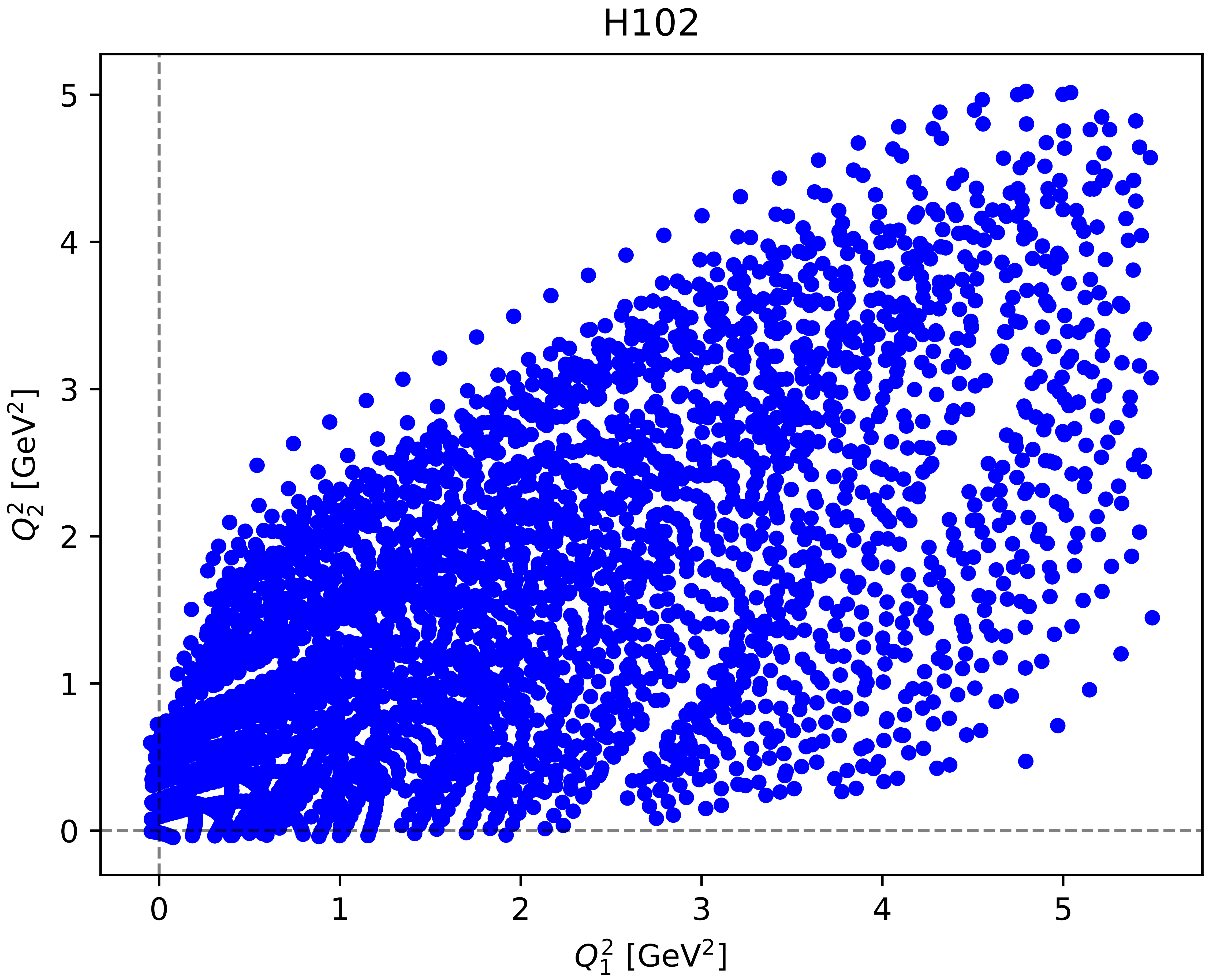

Lattice QCD: correlation functions

How the operator is discretised on the lattice?

- Ensembles ll (local local): needs a renormalization constant.
- Straightforward discretisation of the continuum operator at a lattice site.

- Ensembles lc (local conserved): No renormalization needed since is conserved on the lattice.
- Involves links connecting neighbouring sites.

Uncertainties everywhere

Nothing is certain in life.

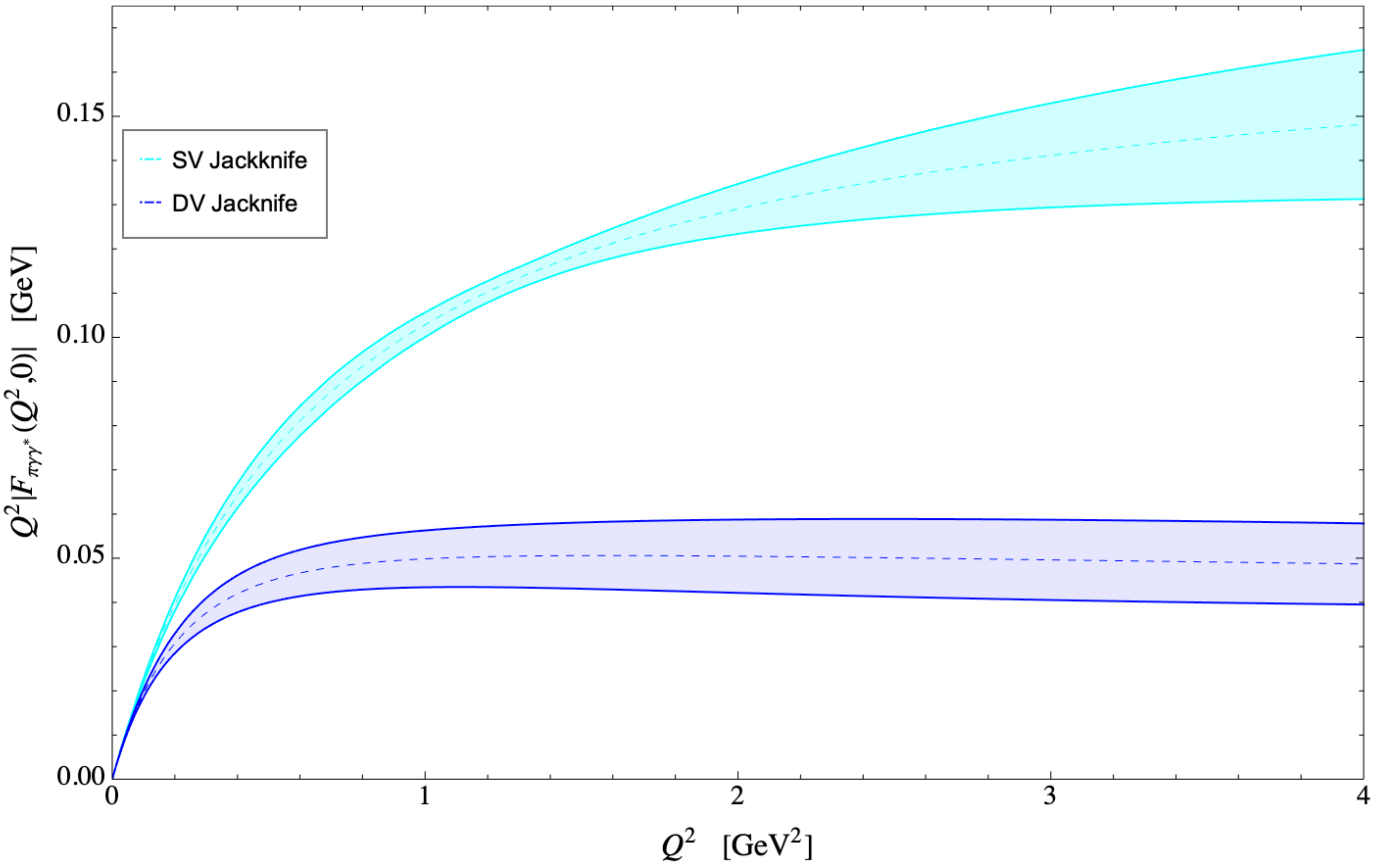

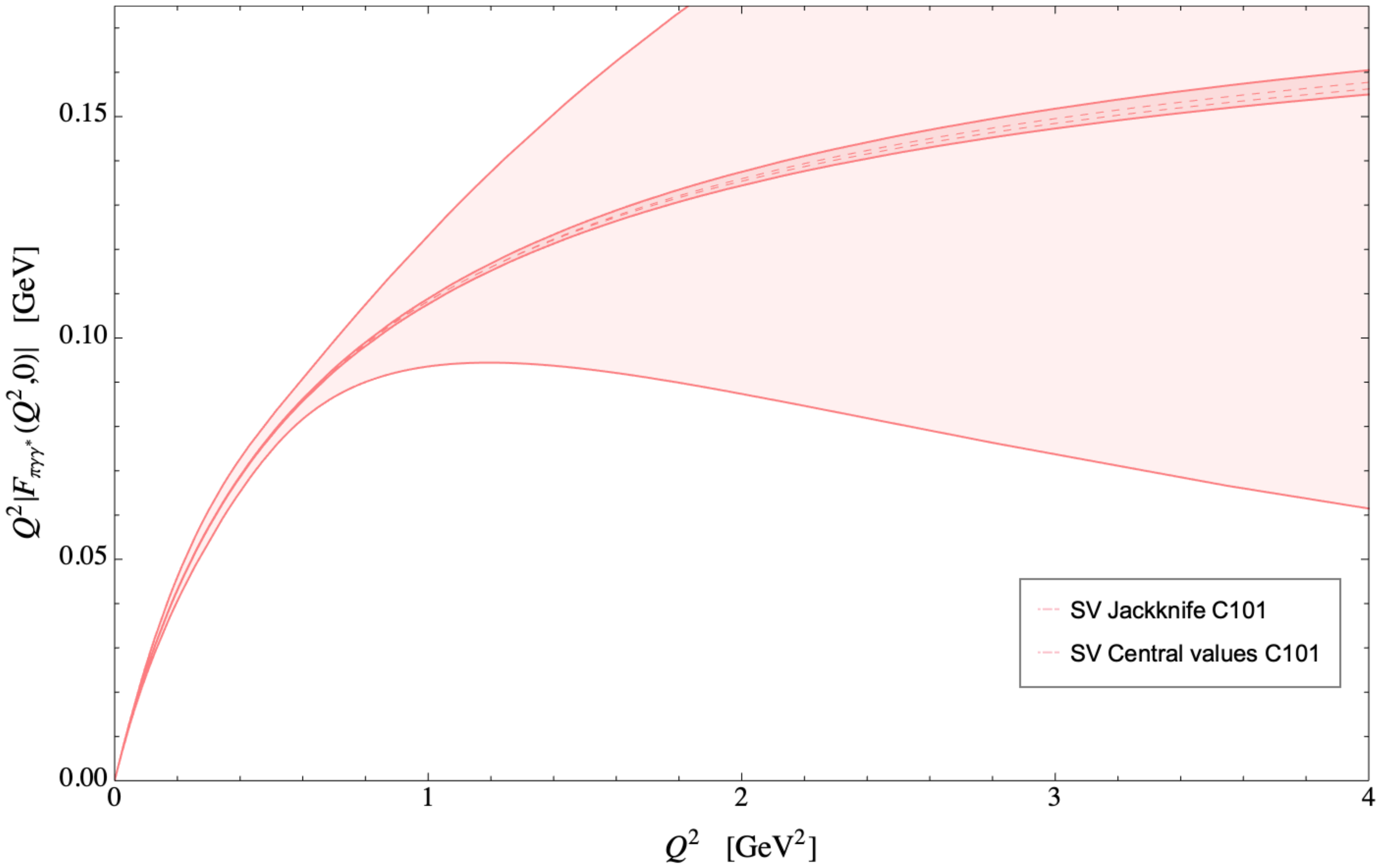

PSEUDOSCALAR-POLE CONTRIBUTION

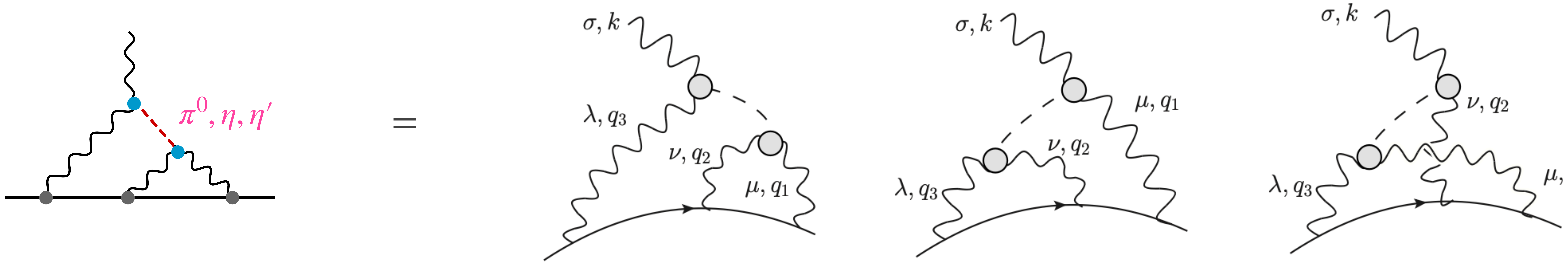

$$a_\mu^{P\text{-pole}} = \left(\frac{\alpha}{\pi}\right)^3 \int dQ_1 dQ_2 d\tau \Big[w_1(Q_1, Q_2, \tau)\, F_{P\gamma^*\gamma^*}(-Q_1^2, -Q_3^2) F_{P\gamma^*\gamma}(-Q_2^2, 0)$$
$$+ w_2(Q_1, Q_2, \tau)\, F_{P\gamma^*\gamma^*}(-Q_1^2, -Q_2^2) F_{P\gamma^*\gamma}(-Q_3^2, 0) \Big]$$

on-shell pseudoscalar transition form factors (TFFs)

kernel functions are peaked at low energies

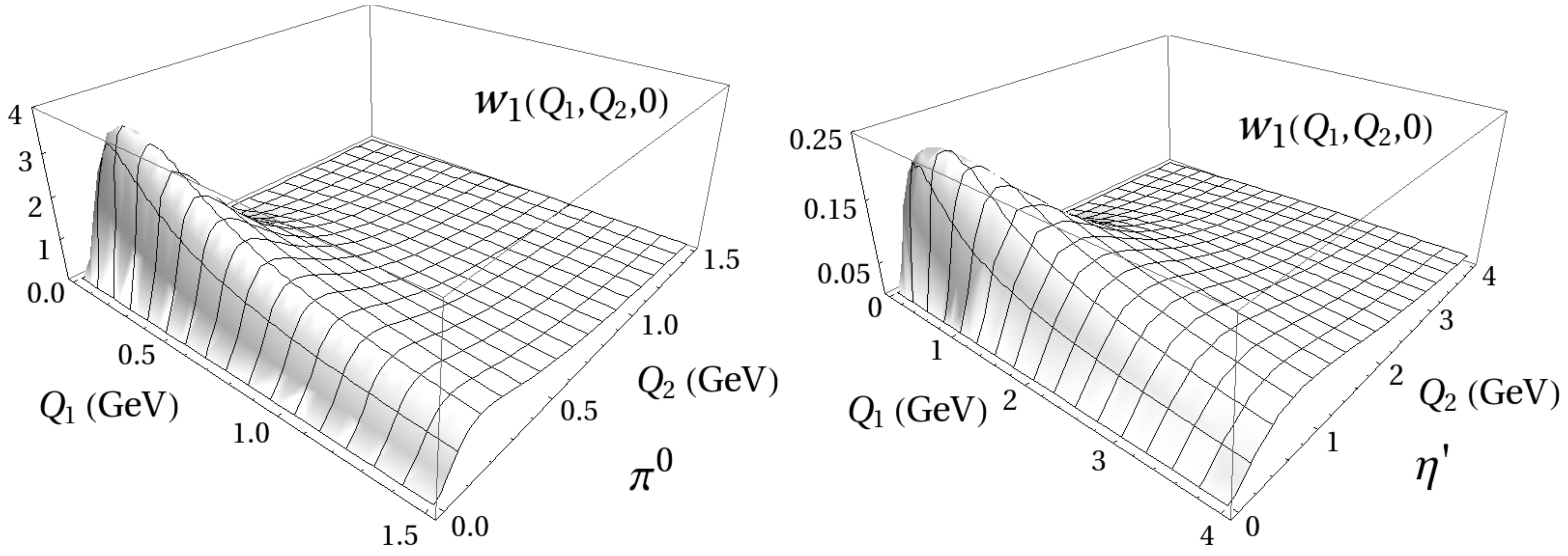

Figure 58: Weight function $w_1(Q_1, Q_2, 0)$ for π^0 (left) and η' (right); cf. Eq. (4.19). Reprinted from Ref. [19].

SLIDE COURTESY OF F. HAGELSTEIN.

ETA & ETA’ TFF

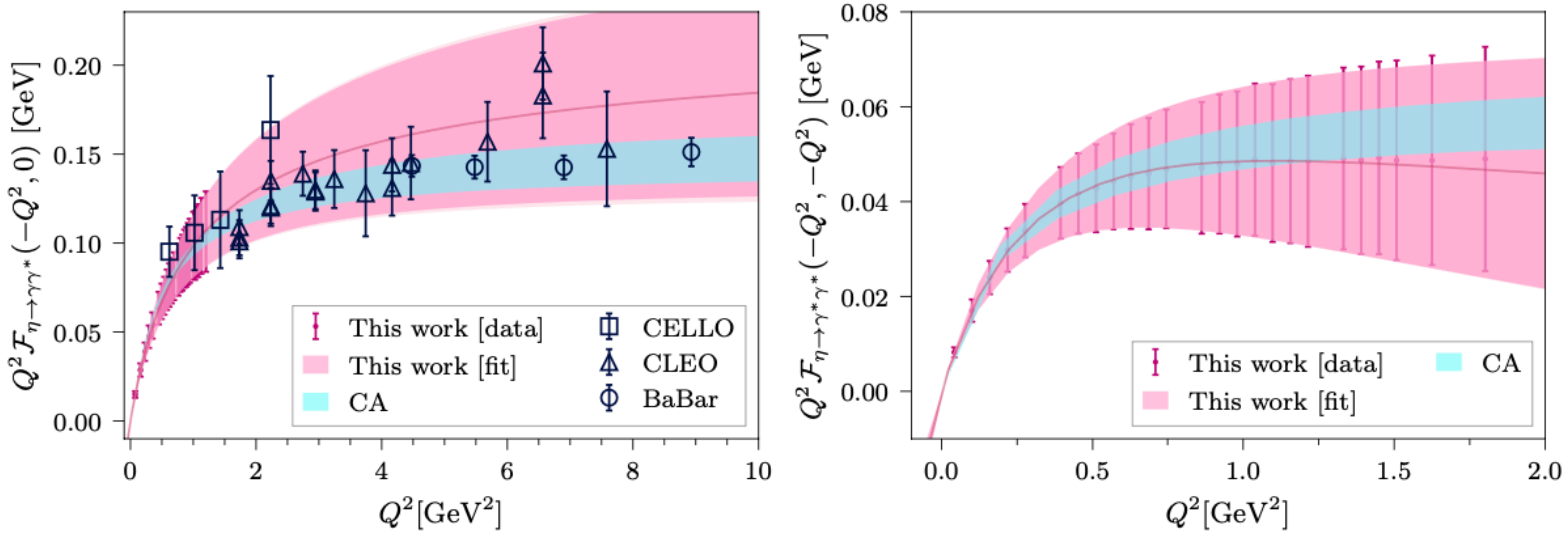

Figure 73: The η TFF from the ETM collaboration in the single-virtual (left) and double-virtual (right) kinematics [570]. The result, obtained at a single lattice spacing, is compared with experimental results and the Canterbury estimate (cyan bands).

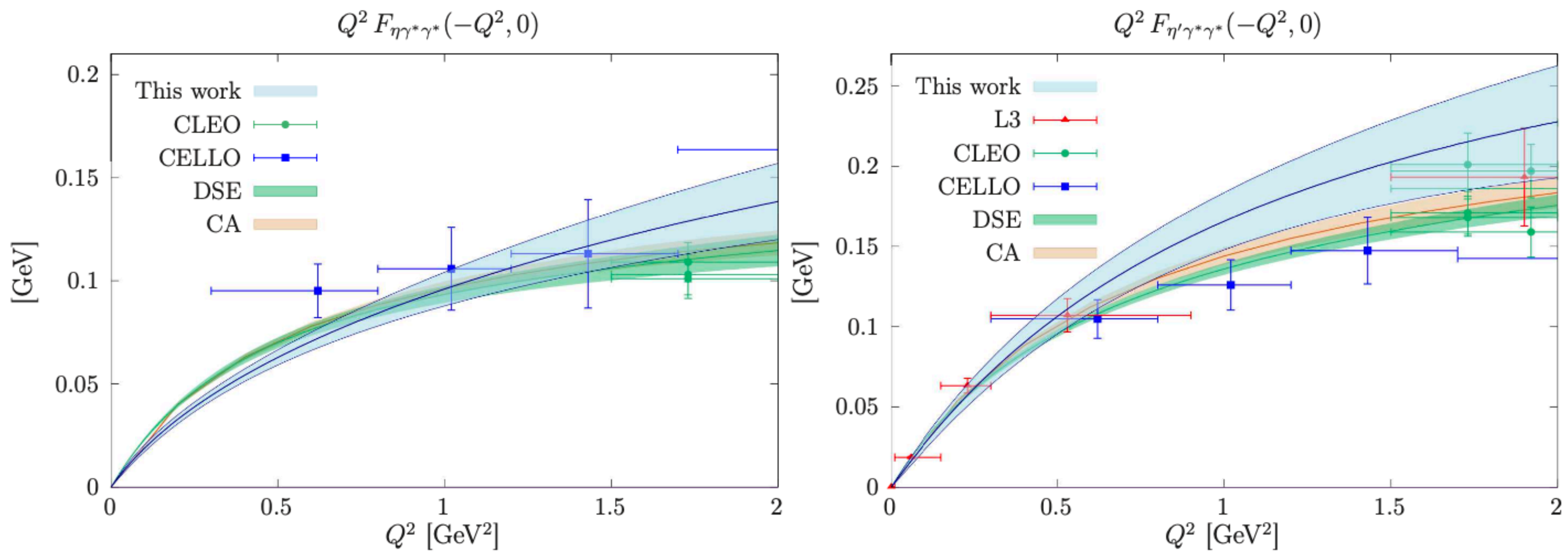

Figure 74: The η (left) and η' (right) single-virtual TFFs from the BMW collaboration at the physical point and in the continuum limit. The Canterbury approximant (CA) result is extracted from Ref. [34] and the Dyson–Schwinger equation (DSE) result comes from Ref. [37]. Measurements from CELLO [559], CLEO [560], and L3 [561] are shown for comparison. Figure from Ref. [571].

SLIDE COURTESY OF F. HAGELSTEIN.